

*Citation for published version:*

Hussain, A, Calabria-Holley, J & Lawrence, R 2019, 'Resilient hemp shiv aggregates with engineered hygroscopic properties for the building industry', *Construction and Building Materials*, vol. 212, pp. 247-253. <https://doi.org/10.1016/j.conbuildmat.2019.03.327>

*DOI:*

[10.1016/j.conbuildmat.2019.03.327](https://doi.org/10.1016/j.conbuildmat.2019.03.327)

*Publication date:*

2019

*Document Version*

Peer reviewed version

[Link to publication](#)

*Publisher Rights*

CC BY-NC-ND

**University of Bath**

**Alternative formats**

If you require this document in an alternative format, please contact:  
[openaccess@bath.ac.uk](mailto:openaccess@bath.ac.uk)

**General rights**

Copyright and moral rights for the publications made accessible in the public portal are retained by the authors and/or other copyright owners and it is a condition of accessing publications that users recognise and abide by the legal requirements associated with these rights.

**Take down policy**

If you believe that this document breaches copyright please contact us providing details, and we will remove access to the work immediately and investigate your claim.

# Resilient hemp shiv aggregates with engineered hygroscopic properties for the building industry

Atif Hussain\*, Juliana Calabria- Holley, Mike Lawrence, Yunhong Jiang

BRE Centre for Innovative Construction Materials, Department of Architecture and Civil Engineering, University of Bath, Bath BA2 7AY, UK

\*Corresponding Author: Atif Hussain ([A.Hussain@bath.edu](mailto:A.Hussain@bath.edu))

## Abstract

This study focuses on the surface treatment of an extremely hydrophilic natural plant material, hemp shiv, using a functionalised silica based coating to provide hydrophobicity while retaining its moisture buffering ability. The chemical composition and physical structure of bio-based materials results in their extremely hydrophilic behaviour. In this work, a simple one step coating process was used to enhance the water-repellence of hemp shiv without compromising its ability to adsorb and release moisture. The coating modified the morphology and surface roughness of hemp shiv providing a hydrophobic surface having a water contact angle of 118° and reduced the bulk water absorption by 250% over 24 hours. Mercury intrusion porosimetry (MIP) showed that the treatment refined the pore size distribution of hemp shiv, reducing the size of larger pores but not completely blocking the smaller pores thereby allowing hemp shiv to buffer moisture. Fourier-transform infrared spectroscopy (FTIR) revealed the chemical composition was modified by the coating, reducing the hydroxyl groups. Hemp shiv aggregates treated with functionalised silica based coating show potential for the development of robust lightweight building materials with enhanced hydrophobicity.

**Keywords:** hemp shiv; bio-based aggregates; hygroscopic; moisture buffering; hydrophobicity; surface engineering.

## 1. Introduction

Bio-based aggregates in the building industry has become popular due to their lower embodied energy, lower CO<sub>2</sub> emissions and good hygrothermal properties reducing the energy demands of buildings [1]. Hemp shiv is the woody core obtained from the stem of the hemp (*Cannabis Sativa* L.). Hemp shiv based composites have been actively researched due to their high moisture buffering and good thermal insulation properties providing a comfortable indoor living environment [2,3]. The moisture buffering property, absorb and release moisture at dynamic relative humidity levels, of hemp shiv is associated with its pore structure. Hemp shiv has a dry bulk density of  $107 \pm 3 \text{ kg/m}^3$  [4] and porosity of 76-78% [5] tending to absorb huge volume of water when compared with other plant materials [6]. The chemical composition of industrial hemp shiv are: 44-46% cellulose, 18-27% hemicellulose, 22-28% lignin, 1-6% extractives and 1-2% ash [7,8] . Cellulose forms the main structural part of hemp shiv containing free hydroxyl groups which are responsible for the extreme hydrophilicity. As a result, hemp shiv based building composites have extremely long drying times when mixed with lime [9], or they have poor interfacial adhesion with the polymeric matrix [10]. Moisture sensitivity also results in microbial growth causing degradation of the aggregate cell wall and deterioration of the composite durability [11].

The wetting behaviour of any solid surface is governed by the surface chemical composition and its geometric structure [12,13]. The interaction between surface roughness and chemistry is actively researched for improving the hydrophobic properties of plant based materials. One of the mechanisms to enhance the hydrophobicity of plant based materials involves altering the chemical composition by blocking the cell wall hydroxyl group. Some of the approaches include addition of silanes [14,15], acetylation [16] or in situ polymerization [17] that involve chemical modification of the aggregate cell wall. Other approaches that can enhance surface roughness and hydrophobicity of the material include sol-gel coatings, plasma treatment or lithography. The sol-gel technique can be carried at room temperature and it is widely used for enhancing surface hydrophobicity by depositing coatings with low surface energy and

increased roughness [18]. Sol-gel coatings have been used on various bio-based materials for improving their hydrophobicity [14,19–21] however there is limited knowledge on the impact of sol-gel coatings on hemp shiv. Sol-gel treatment has also proven to improve the fire resistance and reduce the flammability of cellulose based materials [22].

This work focuses on modification of hemp shiv surface using a functionalised silica based coating to enhance to hydrophobicity of hemp shiv without compromising its moisture buffering capacity. Our work reports the application of a breathable coating on hemp shiv using a simple one step process. The objective of this work was to investigate the effect of a hydrophobic silica coating on the porosity, moisture buffering ability and surface morphology of hemp shiv.

## 2. Experimental

### 2.1 Materials

The hemp shiv aggregates (Figure 1) were received from an agricultural cooperative CAVAC, France. Tetraethyl orthosilicate (TEOS, 98%), nitric acid ( $\text{HNO}_3$ , 70%), hexadecyltrimethoxysilane (HDTMS, 85%) and absolute ethanol were received from Sigma-Aldrich.



*Figure 1. Hemp shiv aggregates used in this study.*

## **2.2 Coating preparation**

The coating was prepared by hydrolysis and condensation of TEOS in water and ethanol and nitric acid was added as the catalyst. The coating formulation was 1M of TEOS, 4M water, 4M ethanol and 0.005M nitric acid. The solution was stirred using a magnetic stirrer for 30 minutes at 300 rpm and 40 °C. After the preparation of silica formulation, 1 wt. % of HDTMS was added as the hydrophobic agent and the sol was stirred for another 20 minutes at 300rpm. The pH of the prepared sol was measured to be 1.92.

The prepared sol aged in a sealed vial for 48 hours at 20 °C. Hemp shiv aggregates were immersed in the sol for 10 min and then carefully placed on a Petri dish for drying at room temperature 20 °C for an hour. The aggregates were then dried at 80 °C for an hour in a laboratory oven. The treated samples were stored in a sealed vial for further sample characterisation. The treated samples had an average mass gain of 18% due to the deposition of the silica coating on the hemp shiv. For calculating the amount of residual water, the treated samples were vacuum sealed in a glass tube, heated at 150°C overnight and then weighed. The residual water content was found to be 5 wt. % for coated hemp shiv samples. The silica glass was prepared by aging the sol in a sealed vial for 48 hours at 20 °C and then placed in oven at 80 °C for at least 120 hours to undergo dehydration. The gel time of the prepared sol was 101 days when stored in a sealed vial at 20 °C. The coating formulation and the dipping time has been reported to deposit uniform crack free coatings on hemp in our recently published paper [23].

## **2.3 Contact Angle Measurements**

The determination of water contact angle (WCA) was performed by a contact angle meter (First Ten Ångströms USA, FTA200 series) using the static sessile drop method. The WCA readings were taken for a minimum of 3 different samples. The water droplets used during the test had a volume of 5µl. The recorded images were analysed by FTA32 Video 2.0 software. The experiment was performed at room temperature ( $20 \pm 1$  °C).

## **2.4 Water absorption test**

Prior to the test, the samples were dried overnight in an oven at 80 °C and then weighed for recording the initial mass. The samples were placed in beaker containing water and since they have a density lower than water, the samples floated and only one side of the shiv was in contact with water. Therefore, the water uptake was mainly due to capillary behaviour. The readings were taken at frequent intervals for 24 hours, in which the sample was taken out of water using a tweezer, shaken off to remove any visible surface water and then weighed within 30s. Mass readings were recorded to the nearest 0.1 mg and an average of three readings from different samples was reported as the final measurement [24,25].

## **2.5 Dynamic vapour sorption**

For the analysis of the adsorption-desorption isotherm in response to varying humidity levels, a dynamic vapour sorption equipment DVS Advantage, SMS, UK was used. The test protocol was adopted from previous studies [24,26]. The samples weighed around 15 mg and experiment temperature was maintained at 23 °C. The relative humidity (RH) was increased in steps from 0-90% and then decreased back to 0%. The actual and target RH, sample mass and running time were continuously recorded during the experiment.

The data obtained from the isotherms was used to calculate the moisture content of the samples at any given RH using the following equations:

$$MC = \frac{m_2 - m_1}{m_1} \times 100 \quad (1)$$

$$MC_R = \frac{m_2 - m_1}{m_0} \times 100 \quad (2)$$

Where MC is the measured equilibrium moisture content of the sample;  $MC_R$  is the reduced equilibrium moisture content of the sample before coating;  $m_0$  is mass of oven dried uncoated shiv sample;  $m_1$  is the mass of oven dried coated shiv sample;  $m_2$  is the mass of shiv sample at any given RH. Three cycles of adsorption-desorption were run for each sample and the second cycle was reported.

## **2.6 Scanning Electron Microscopy**

Photomicrographs of the samples were captured using a scanning electron microscope (SEM), JEOL Corporation - Japan Model JSM-6360 operating at 25 kV. The samples were gold coated to obtain high magnification of morphology and texture.

## **2.7 Surface Roughness**

For measurement of sample surface roughness, a 3D optical profilometer, Bruker Nano GmbH ContourGT-K series, Germany was used in non-contact mode. The area analysed for each test was 0.25\*0.30 mm<sup>2</sup> and magnification was set to 20X. The data was analysed by Vision 64 software and the surface roughness was calculated. The test was performed for at least 3 different samples and the average value was reported.

## **2.8 Fourier transform infrared (FTIR) spectroscopy**

For identification of the chemical bonds, FTIR analysis was performed with a PerkinElmer FTIR spectrometer, Model Frontier. Transmittance spectra were recorded in the range of 4000-600 cm<sup>-1</sup> with a resolution of 2 cm<sup>-1</sup> and 10 scans were run for each test. Hemp shiv samples were tested as individual pieces whereas the silica glass sample was crushed to powder form and then mixed with potassium bromide to form pellets.

## **3. Results**

The water contact angles were recorded from 0-60 seconds of contact between the droplet and the hemp shiv surface. From Figure 2, it was observed that hemp shiv surface that have not been coated have highly hydrophilicity. The initial contact angle was 79° and the droplet sinks into the bulk of the sample completely in less than 20 seconds. On the other hand, the sol-gel coated samples have an initial contact angle of 118° making the surface hydrophobic. The contact angle remains stable over 60 seconds of contact.

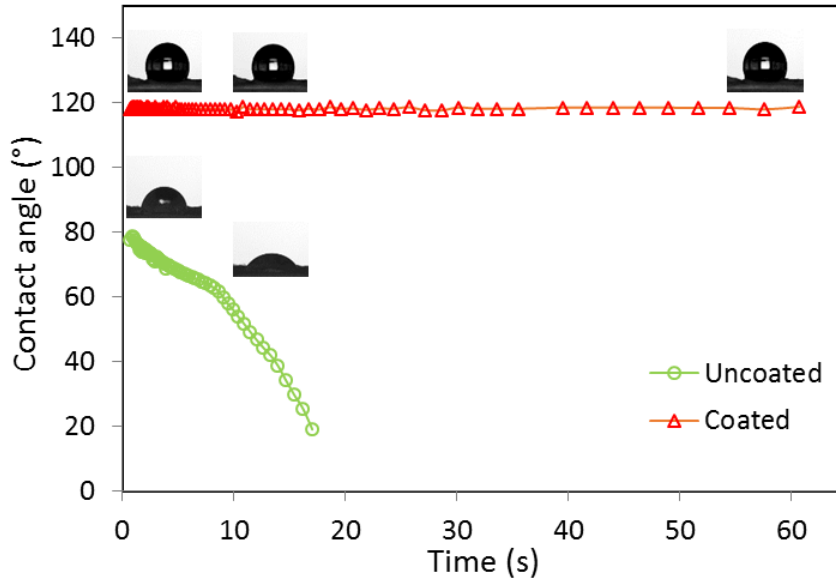


Figure 2. Water contact angles of coated and uncoated hemp shiv over time.

Water absorption (WA %) measures the relative percentage increase in mass due to the retention of water within the bulk of the sample. It is calculated using the following equation:

$$WA \% = \frac{\text{Sample wet weight} - \text{Sample dry weight}}{\text{Sample dry weight}} \times 100 \quad (3)$$

Considering the mass increase of hemp shiv due to the coating, equation (3) can be modified to calculate the reduced water absorption ( $WA_R$  %) as follows:

$$WA_R \% = \frac{\text{Coated sample wet weight} - \text{Coated sample dry weight}}{\text{Uncoated sample dry weight}} \times 100 \quad (4)$$

Figure 3 shows the absorption of water for coated and uncoated hemp shiv samples over 24 hour period. It was observed that within the initial few minutes of contact with water, hemp shiv can absorb a huge volume of water corresponding the significantly high mass increase. Uncoated hemp shiv shows extremely high water absorption reaching up to 4 times its initial mass after 24 hours. This tendency of absorbing water is mainly caused by the hydrophilic behaviour of hemp shiv and its highly porous structure. Hemp shiv treated with the silica coating shows a significant reduction in water absorption by almost 250%. The treated shiv sample absorbs water only 1.5 times its initial mass over 24 hours. From equation (4), the



reduced water absorption of the coated hemp shiv was calculated to be 1.8 times its initial mass which is still significantly lower than the water absorption of uncoated shiv by 220%.

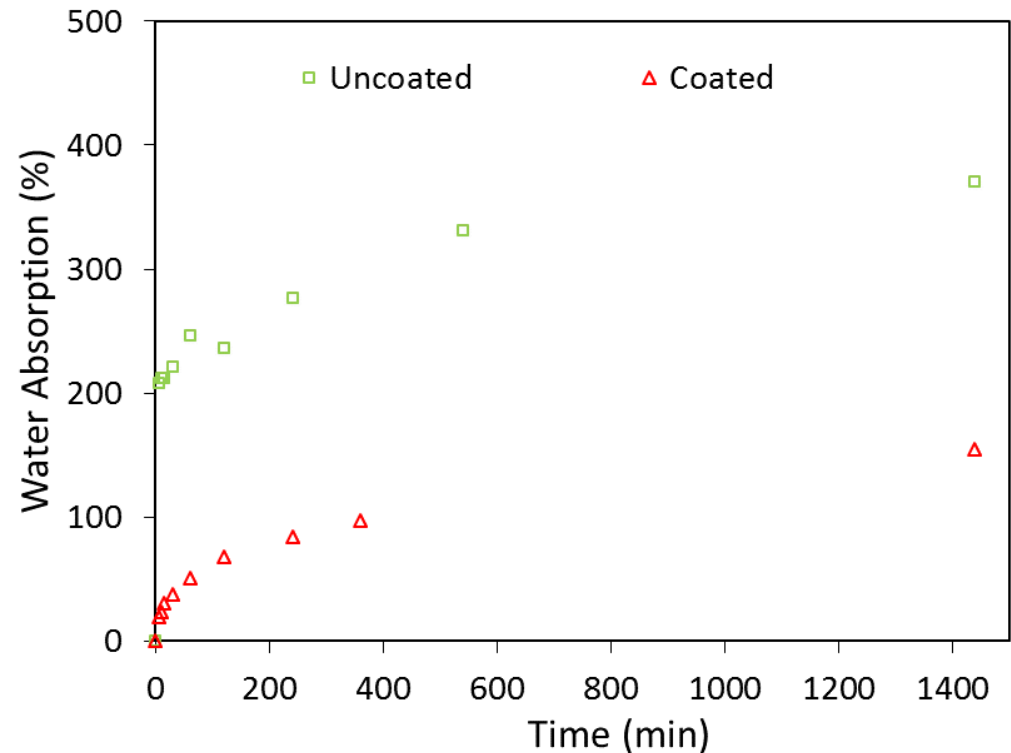
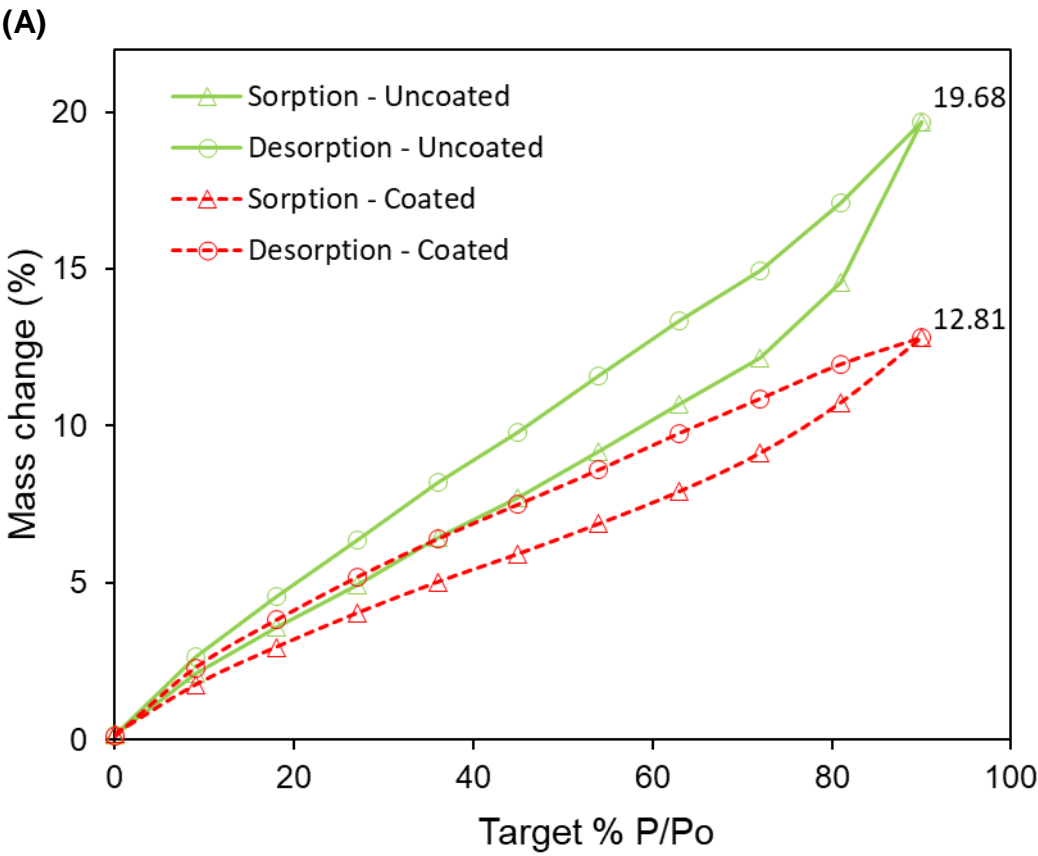


Figure 3. Water absorption of coated and uncoated hemp shiv samples.

The sorption isotherm of coated and uncoated hemp shiv was determined over a RH range 0-90%. It was observed the coating lowered the measured moisture content (MC) in the isotherm. The coating decreased the measured MC of the hemp shiv sample by 30%. Coated shiv showed a maximum measured MC of 12.81% at the highest humidity level of 90% whereas uncoated hemp shiv had a measured MC value of 19.68 % at 90 % relative humidity level as seen in Figure 4a. It has been reported that the water molecules were adsorbed on the surface of hemp shiv linked through hydrogen bonds [27].

It should be noted that the coating increases the mass of hemp shiv and therefore the reduced moisture content ( $MC_R$ ) of the coated shiv was calculated to be 15.12%. The  $MC_R$  of uncoated shiv remains the same as its MC which is 19.68% which means that the moisture adsorption capacity of the coated shiv is not significantly different than the uncoated shiv. The fact that

196 the coating increases the mass of the shiv, equations (1) and (2) show that for uncoated hemp  
197 shiv  $MC = MC_R$  but for coated shiv  $MC < MC_R$  [24,28].  
198



199  
200

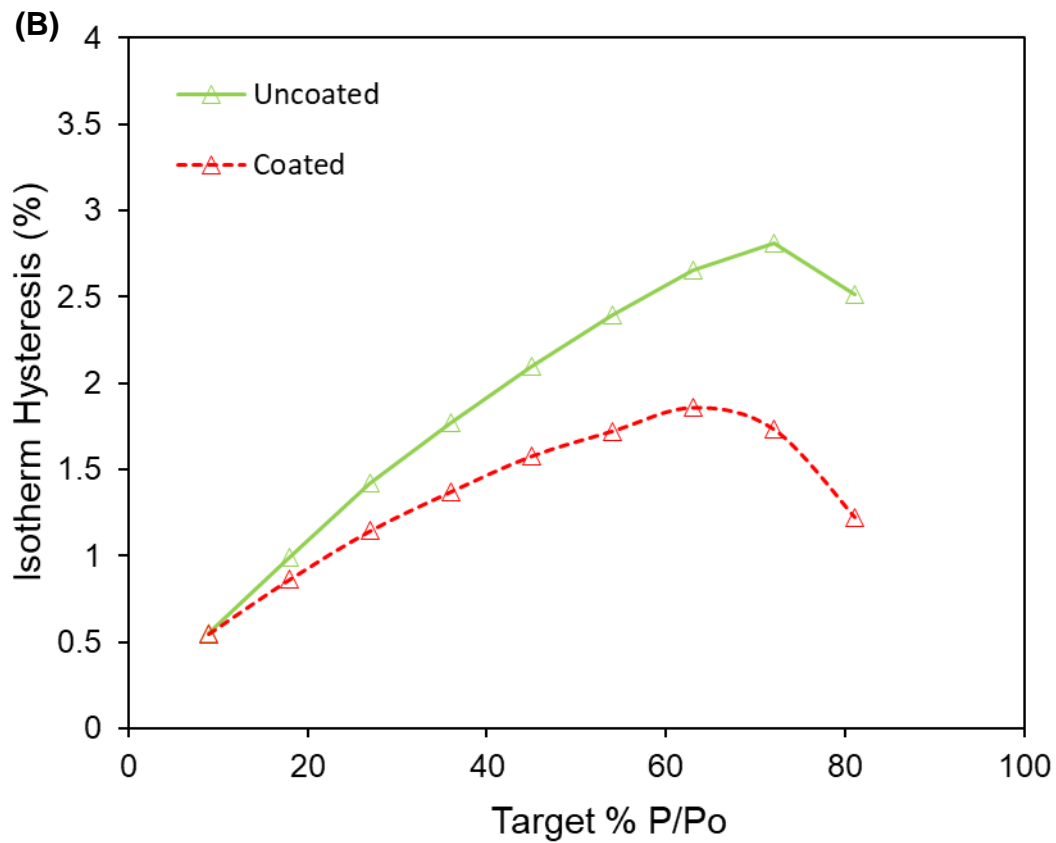


Figure 4. (A) Sorption isotherms; (B) isotherm hysteresis curves of uncoated and coated samples.

The hysteresis values between adsorption and desorption curves of uncoated and coated shiv are presented in Figure 4b. It can be seen from the hysteresis curves that coated shiv shows lower hysteresis when compared to uncoated shiv. It was observed that the difference in hysteresis between coated and uncoated shiv increased at each higher RH step.

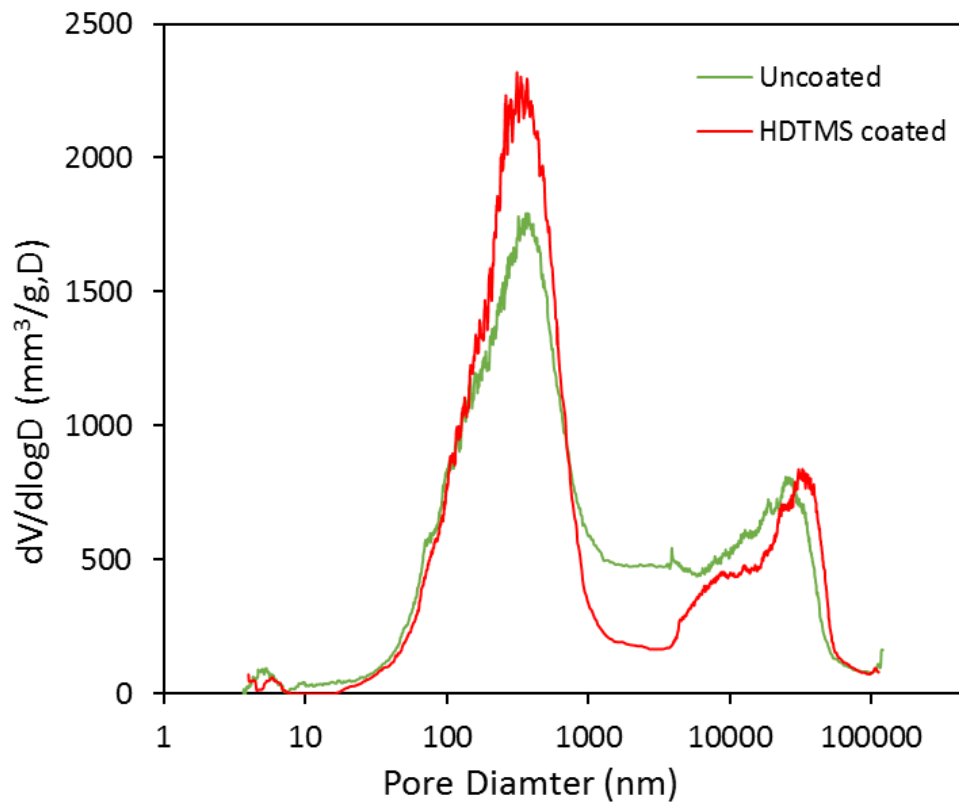
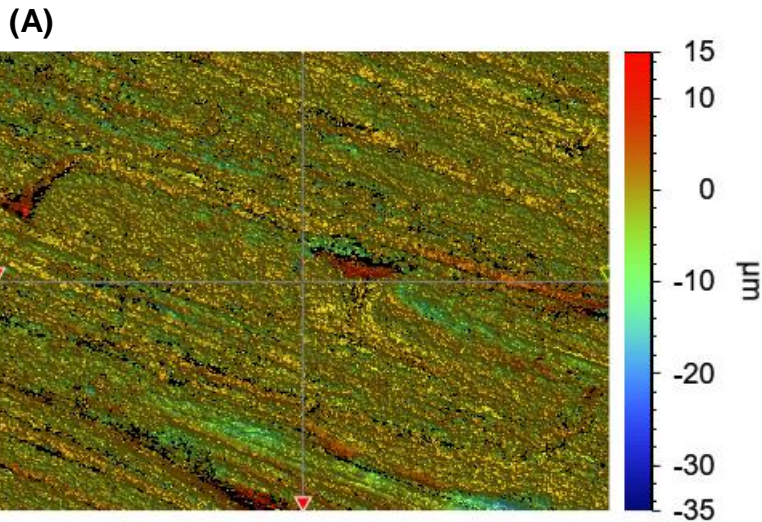


Figure 5. Pore size distribution of uncoated and coated hemp shiv.

The pore size distribution of uncoated and coated shiv is given in Figure 5. The overall porosity of hemp shiv is unaffected by the coating and both samples have a porosity of  $78 \pm 0.7\%$ . The cumulative pore volume is found to be similar as well,  $2428 \text{ mm}^3/\text{g}$  and  $2377 \text{ mm}^3/\text{g}$  for uncoated and coated samples respectively. Figure 5 shows that the coating reduced the diameter of the larger pores, mainly in the range of  $1 \text{ }\mu\text{m}$  to  $10 \text{ }\mu\text{m}$ . The pores over  $50 \text{ }\mu\text{m}$  remain unaffected by the coating suggesting that the layer of coating deposited is very thin and in the nanometer scale.

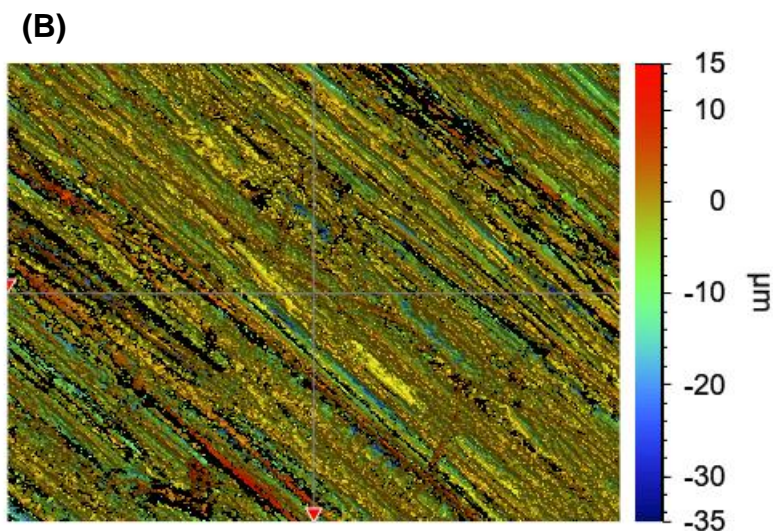
Another observation from Figure 5 is that the coated shiv has increased number of smaller pores in the range of  $100\text{-}800 \text{ nm}$  compared to the uncoated shiv. The overall porosity remaining the similar for both samples suggest that the overall pore volume is not reduced but only the pores have been refined from micron size to nano size.

226



227

228



229

230 *Figure 6. Surface roughness profiles of (a) uncoated; (b) coated shiv.*

231

232 The surface roughness of uncoated and coated hemp shiv samples was analysed by the  
233 software Vision64 and a Robust Gaussian Filter (ISO 16610-31 2016) was applied. The  
234 anatomical influence can be reduced with the help of such filters and the roughness profile can  
235 be optimised for surface evaluation of the sample [29,30]. Moreover, when analysing deep  
236 valleys on the sample surface, the robust Gaussian filter does not produce distortions that  
237 maybe formed by other filters [31]. The mean surface roughness ( $S_a$ ) is the most widely used  
238 parameter for describing the variations in surface height and was calculated according to ISO  
239 4287 (1997). The 3D roughness profile for uncoated and coated hemp shiv surfaces is shown

in Figure 6. It was observed that the coating enhanced the surface roughness of the samples with a mean  $S_a$  value of 2.07  $\mu\text{m}$  compared to uncoated shiv having a mean  $S_a$  value of 1.79  $\mu\text{m}$ .

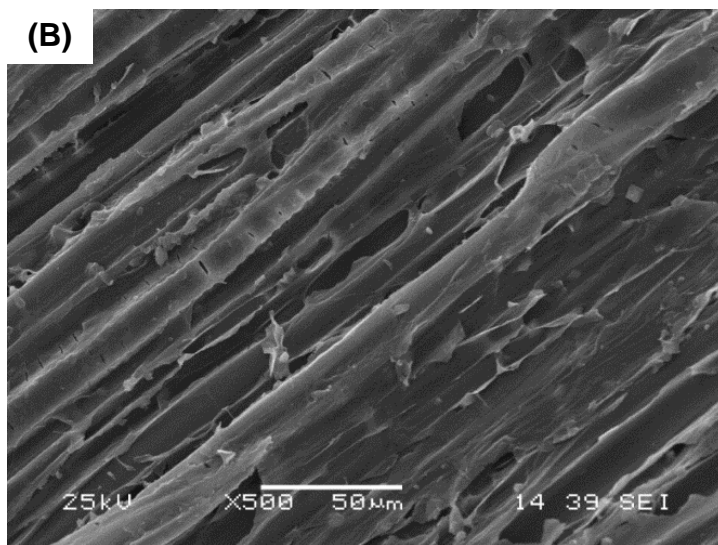
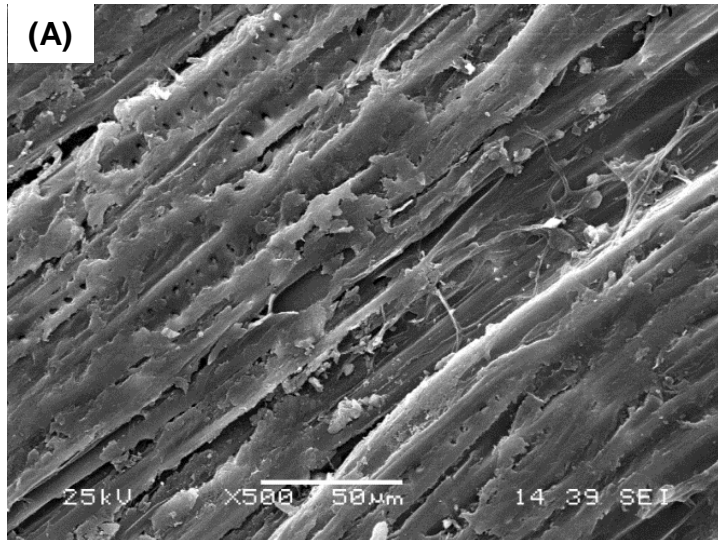


*Figure 7. SEM micrographs showing (A) uncoated; (B) coated hemp shiv surface.*

Morphological characterisation cannot be performed by roughness parameters alone and therefore microscopic examination is advantageous for better surface evaluations. The surface morphology of the uncoated and coated surfaces was further evaluated using SEM. From SEM micrographs in Figure 7, it can be seen that the coating has been uniformly deposited over the hemp shiv surface without significantly modifying its microstructure.

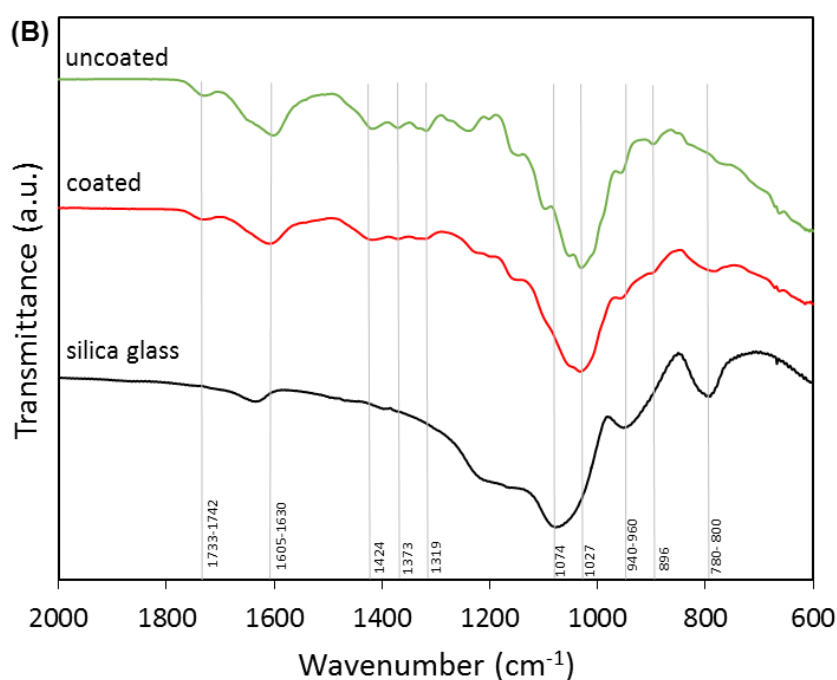
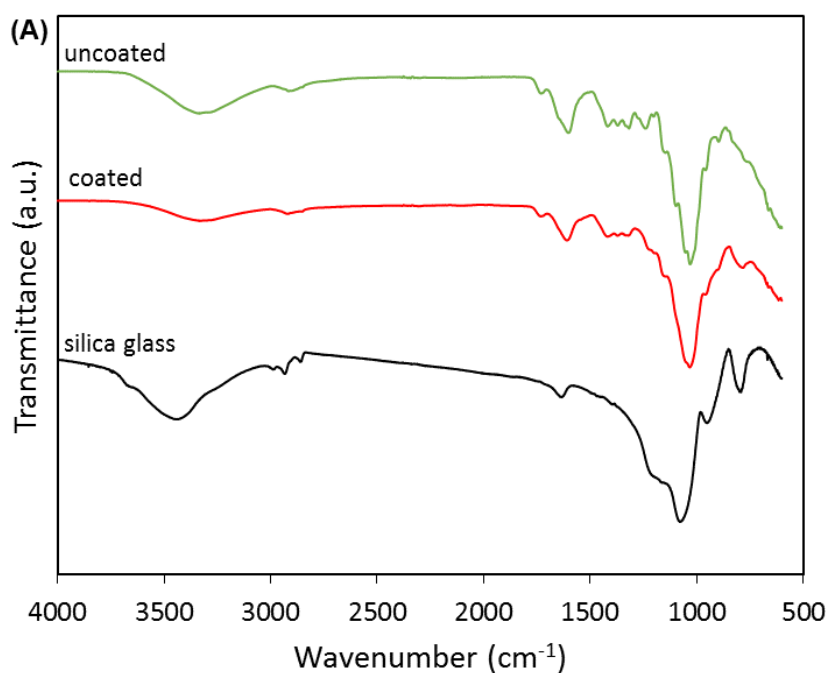


Figure 8. FTIR spectra of silica, coated and uncoated shiv samples for (A) 600-4000  $\text{cm}^{-1}$  region; (B) 600-2000  $\text{cm}^{-1}$  region.

The FTIR spectra of silica glass, coated and uncoated hemp shiv is shown in Figure 8. Free water bands corresponding to the wave number interval 3300-3400  $\text{cm}^{-1}$  have been reduced in the coated shiv samples as seen in Figure 8A. This decrease in signal indicates that the hydrophobicity of the shiv has been enhanced by the deposition of the silica coating. The peaks

at 2918  $\text{cm}^{-1}$  and 2851  $\text{cm}^{-1}$  correspond to C-H vibration and  $\text{CH}_2$  stretching from polysaccharides, wax and the alkyl chains. The peaks at wavenumber 1605-1630  $\text{cm}^{-1}$  correspond to adsorbed water. From figure 8B, it was observed that coated shiv showed lower peak intensity corresponding to wavenumbers 1742-1733  $\text{cm}^{-1}$  ( $\text{C}=\text{O}$  from hemicellulose), 1424  $\text{cm}^{-1}$  ( $\text{CH}_2$ ,  $\text{C}=\text{C}$  from cellulose and lignin), 1373  $\text{cm}^{-1}$  (C-H from cellulose), 1319  $\text{cm}^{-1}$  (C-C,  $\text{CH}_2$  from cellulose and lignin), 1027  $\text{cm}^{-1}$  (C-C, C-OH, C-H from hemicellulose) and 896  $\text{cm}^{-1}$  (C-O-C glycosidic bonds from polysaccharides). The deposition of the silica coating can be confirmed by wavenumbers 940  $\text{cm}^{-1}$  associated with Si-OH bonds vibration and 780  $\text{cm}^{-1}$  incomplete hydrolysis of TEOS molecules. The peak at 1000-1100  $\text{cm}^{-1}$  for the silica glass corresponds to Si-O-Si bonds.

#### 4. Discussion

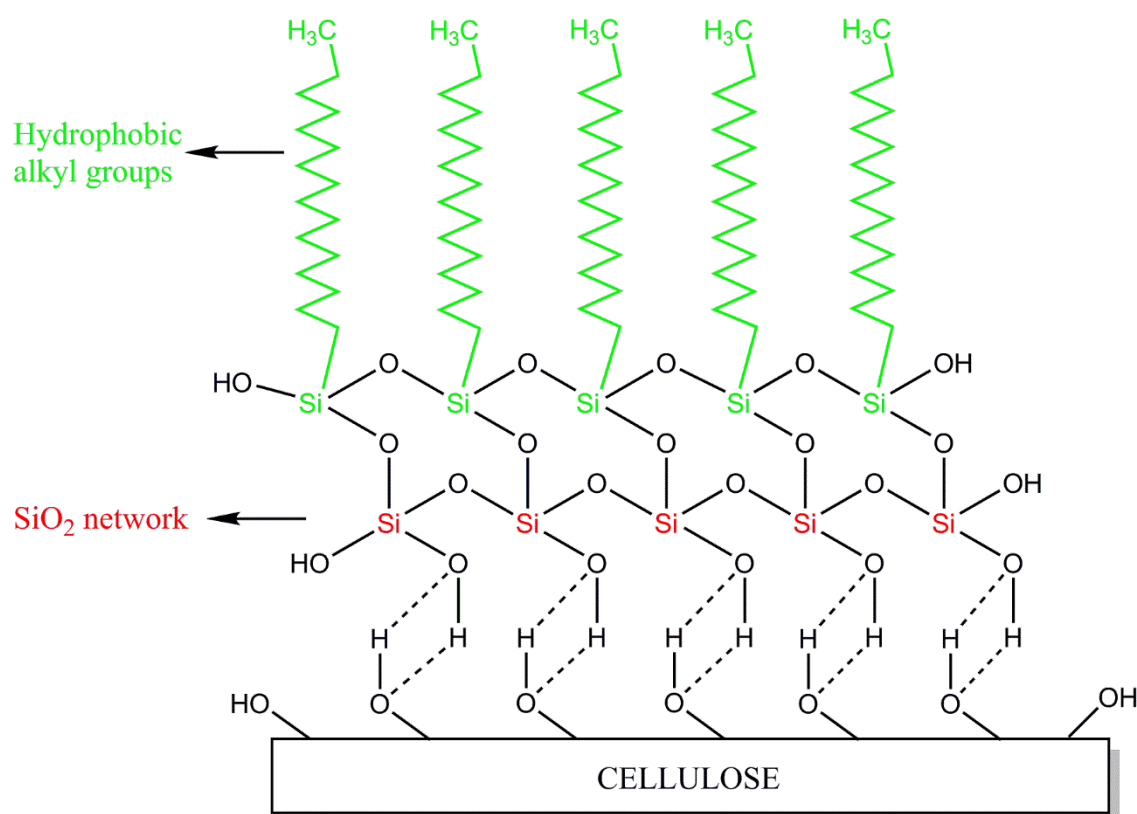


Figure 9. Schematic illustration of sol-gel deposition on hemp shiv surface.

The silica based coatings were prepared through the sol-gel process and HDTMS was added as the hydrophobic agent in the sol formulation. A schematic illustration of deposition of the



coating on hemp shiv surface through the hydroxyl sites of cellulose is presented in Figure 9. During the sol-gel process, hydrolysis and condensation of TEOS forms a silica ( $\text{SiO}_2$ ) network. The HDTMS molecules self-assemble replacing the hydroxyls on silica network and long alkyl chains ( $-\text{Si}-\text{C}_{16}$ ) are attached on the silica network. Coating the hemp shiv results in attachment of the silica network to the shiv surface through the cellulose hydroxyl groups which are also chemically linked to the alkyl groups responsible for providing hydrophobicity to the shiv surface.

The surface wettability of hemp shiv is controlled by the chemical composition and the morphology. Hemp shiv tends to absorb huge volume of water within a few minutes of contact as hydroxyl sites are present in large numbers on its surface and in this structure. Moreover, the extreme hydrophilicity of hemp shiv can also be assigned to its high roughness profile. Surface roughness can cause an increase or decrease in the water contact angle depending on the nature of the material. Roughness is defined as the ratio between the actual surface area to the geometrically projected area. Higher surface roughness results in increased hydrophilicity for hydrophilic materials but for hydrophobic surfaces, higher surface roughness enhances the hydrophobicity of the material. For a hydrophilic surface, high surface roughness provides a large surface area increasing the interaction with a water droplet, thereby providing a low water contact angle. On the other hand, a hydrophobic surface has micro scale protrusions which cannot be filled by the liquid and instead filled by air resulting in higher contact angles [32]. In the present work, the hydrophobicity of the coated hemp shiv surface is due to the self-assembled layer of HDTMS on the silica network reducing the cellulose hydroxyl sites as seen in Figure 9. The surface roughness of the hemp shiv was enhanced due the deposition of the coating. The coated hemp shiv exhibited excellent hydrophobicity with WCA up to  $118^\circ$  due to the combination of enhanced surface roughness and low surface energy of the HDTMS chains. Durability studies on composites made with treated hemp shiv by completely immersing them in water for 24 hours and testing their mechanical performance have been reported in a recent paper [33].

The microstructure of hemp shiv remained unaltered after sol-gel treatment. From SEM results, it was observed that the coating was deposited as a uniform layer and no cracks were observed after drying the shiv. The hydrophobicity of the substrate can be affected by cracks in the coating layer as water molecules can penetrate, wetting the substrate over time. The water absorption results showed that the sol-gel coating layer provided excellent resistance to water due to the hydrophobic functional groups in the coating. The water uptake for the coated hemp shiv was massively reduced within the first few minutes of contact and the water absorption was reduced by 250% over 24 hours when compared to the uncoated shiv.

The high values of moisture adsorption for hemp shiv can be assigned to its chemical composition with a large number of hydroxyl groups being accessible. The lower water vapour sorption values for the coated shiv can be attributed to the hydrophobic alkyl chains present on the coated surface. Modifying the surface of hemp shiv with the silica coating blocked the surface hydroxyl sites and reduced the mass of water adsorbed at high humidity levels. The silica coating interacts with the hemp shiv subsequently lowering its moisture buffering capacity to a limited extent but the coating does not completely block the pores. This is also in agreement with the SEM micrographs showing this coating formulation had least altered the surface morphology of hemp shiv. From the porosity and DVS results, it can be determined that the coated hemp shiv is capable of adsorbing moisture through the smaller pores whereas the water uptake is considerably reduced due to decrease in the larger pores. Coated shiv showed significant reduction in hysteresis by 49% when compared to uncoated shiv at 90% RH. The reduction in hysteresis curves of the coated shiv shows that water is condensed only on the surface and does not go further deep into the bulk of the hemp shiv structure due to the presence of hydrophobic chains.

## 5. Conclusions

Sol-gel technology has been successfully applied for surface modification of hemp shiv enhancing its hydrophobicity while retaining its moisture buffering capacity. A simple one step

coating process has been used to provide a hydrophobicity to a highly hydrophilic bio-based material. The coated surface exhibited excellent hydrophobic properties through the synergistic effect of enhanced surface roughness and modified chemical composition. Uniform crack-free monolayer surface coatings delivered contact angles up to 118° and significantly lowered the water absorption rate. The sol-gel coating does not significantly alter the microstructure of the shiv thereby retaining the ability to adsorb and desorb humidity. Silica coated hemp shiv has the potential to be used as a superior aggregate and mixed with binders to produce water-resistant bio-based building composites.

## **Funding**

The work was supported by the ISOBIO project funded by the Horizon 2020 programme [Grant number 636835 – ISOBIO – H2020-EeB-2014-2015] and the EPSRC Centre for Decarbonisation of the Built Environment (dCarb) [grant number EP/L016869/1]. The contents of this publication are the sole responsibility of the authors and can in no way be taken to reflect the views of the European Union.

## **Acknowledgments**

The authors thank Prof Pierre Blanchet and Dr Diane Schorr for access to 3D profilometer at Université Laval.

## **Data access statement**

All data are provided in full in the results section of this paper.

## **Disclosure statement**

The authors declare that they have no conflict of interest.

## **References**

- [1] M. Lawrence, Reducing the Environmental Impact of Construction by Using Renewable Materials, *J. Renew. Mater.* 3 (2015) 163–174.

- 365 doi:10.7569/JRM.2015.634105.
- 366 [2] E. Latif, M. Lawrence, A. Shea, P. Walker, Moisture buffer potential of experimental  
367 wall assemblies incorporating formulated hemp-lime, *Build. Environ.* 93 (2015) 199–  
368 209. doi:10.1016/j.buildenv.2015.07.011.
- 369 [3] F. Collet, J. Chamoin, S. Pretot, C. Lanos, Comparison of the hygric behaviour of  
370 three hemp concretes, *Energy Build.* 62 (2013) 294–303.  
371 doi:10.1016/j.enbuild.2013.03.010.
- 372 [4] B. Mazhoud, F. Collet, S. Pretot, C. Lanos, Mechanical properties of hemp-clay and  
373 hemp stabilized clay composites, *Constr. Build. Mater.* 155 (2017) 1126–1137.  
374 doi:10.1016/j.conbuildmat.2017.08.121.
- 375 [5] Y. Jiang, M. Lawrence, M.P. Ansell, A. Hussain, Cell wall microstructure, pore size  
376 distribution and absolute density of hemp shiv, *R. Soc. Open Sci.* 5 (2018) 171945.  
377 doi:10.1098/rsos.171945.
- 378 [6] H.R. Kymainen, M. Hautala, R. Kuisma, A. Pasila, Capillarity of flax/linseed (*Linum*  
379 *usitatissimum* L.) and fibre hemp (*Cannabis sativa* L.) straw fractions, *Ind. Crops Prod.*  
380 14 (2001) 41–50. doi:10.1016/S0926-6690(00)00087-X.
- 381 [7] L. Kidalova, N. Stevulova, E. Terpakova, Influence of water absorption on the selected  
382 properties of hemp hurds composites, *Pollack Period.* (2015).  
383 doi:10.1556/Pollack.10.2015.1.12.
- 384 [8] M.R. Vignon, D. Dupeyre, Steam explosion of woody hemp ch nevotte, 17 (1995)  
385 395–404.
- 386 [9] L. Arnaud, E. Gourlay, Experimental study of parameters influencing mechanical  
387 properties of hemp concretes, *Constr. Build. Mater.* 28 (2012) 50–56.  
388 doi:10.1016/j.conbuildmat.2011.07.052.
- 389 [10] J. Gassan, V.S. Gutowski, A.K. Bledzki, About the surface characteristics of natural  
390 fibres, *Surf. Eng.* 283 (2000) 132–139. doi:10.1002/1439-  
391 2054(20001101)283:1<132::AID-MAME132>3.0.CO;2-B.
- 392 [11] S. Marceau, P. Glé, M. Guéguen-Minerbe, E. Gourlay, S. Moscardelli, I. Nour, S.  
393 Amziane, Influence of accelerated aging on the properties of hemp concretes, *Constr.*  
394 *Build. Mater.* 139 (2017) 524–530. doi:10.1016/j.conbuildmat.2016.11.129.
- 395 [12] J. Genzer, K. Efimenko, Recent developments in superhydrophobic surfaces and their  
396 relevance to marine fouling: a review., *Biofouling.* 22 (2006) 339–360.  
397 doi:10.1080/08927010600980223.
- 398 [13] A. Nakajima, K. Hashimoto, T. Watanabe, Recent studies on super-hydrophobic films,  
399 in: *Monatshefte Fur Chemie*, 2001: pp. 31–41. doi:10.1007/s007060170142.
- 400 [14] S. Donath, H. Militz, C. Mai, Wood modification with alkoxysilanes, *Wood Sci. Technol.*  
401 38 (2004) 555–566. doi:10.1007/s00226-004-0257-1.
- 402 [15] U. Benitha Sandrine, V. Isabelle, M. Ton Hoang, C. Maalouf, Influence of chemical  
403 modification on hemp-starch concrete, *Constr. Build. Mater.* 81 (2015) 208–215.  
404 doi:10.1016/j.conbuildmat.2015.02.045.
- 405 [16] M.M. Kabir, H. Wang, K.T. Lau, F. Cardona, Chemical treatments on plant-based  
406 natural fibre reinforced polymer composites: An overview, *Compos. Part B Eng.* 43  
407 (2012) 2883–2892. doi:10.1016/j.compositesb.2012.04.053.

- 408 [17] E. Cabane, T. Keplinger, V. Merk, P. Hass, I. Burgert, Renewable and functional wood  
409 materials by grafting polymerization within cell walls, *ChemSusChem*. 7 (2014) 1020–  
410 1025. doi:10.1002/cssc.201301107.
- 411 [18] J. Song, O.J. Rojas, Approaching super-hydrophobicity from cellulosic materials : A  
412 Review, *Pap. Chem.* 28 (2013) 216–238. doi:10.3183/NPPRJ-2013-28-02-p216-238.
- 413 [19] S. Wang, C. Liu, G. Liu, M. Zhang, J. Li, C. Wang, Fabrication of superhydrophobic  
414 wood surface by a sol-gel process, *Appl. Surf. Sci.* 258 (2011) 806–810.  
415 doi:10.1016/j.apsusc.2011.08.100.
- 416 [20] B. Mahltig, H. Böttcher, Modified silica sol coatings for water-repellent textiles, *J. Sol-  
417 Gel Sci. Technol.* 27 (2003) 43–52. doi:10.1023/A:1022627926243.
- 418 [21] G.Y. Bae, B.G. Min, Y.G. Jeong, S.C. Lee, J.H. Jang, G.H. Koo, Superhydrophobicity  
419 of cotton fabrics treated with silica nanoparticles and water-repellent agent, *J. Colloid  
420 Interface Sci.* 337 (2009) 170–175. doi:10.1016/j.jcis.2009.04.066.
- 421 [22] J. Mastalska-Popławska, M. Pernechele, T. Troczynski, P. Izak, Thermal properties of  
422 silica-coated cellulose fibers for increased fire-resistance, *J. Sol-Gel Sci. Technol.* 83  
423 (2017) 683–691. doi:10.1007/s10971-017-4445-5.
- 424 [23] A. Hussain, J. Calabria-Holley, D. Schorr, Y. Jiang, M. Lawrence, P. Blanchet,  
425 Hydrophobicity of hemp shiv treated with sol-gel coatings, *Appl. Surf. Sci.* 434 (2018)  
426 850–860. doi:10.1016/j.apsusc.2017.10.210.
- 427 [24] A. Hussain, J. Calabria-Holley, Y. Jiang, M. Lawrence, Modification of hemp shiv  
428 properties using water-repellent sol–gel coatings, *J. Sol-Gel Sci. Technol.* 86 (2018)  
429 187–197. doi:10.1007/s10971-018-4621-2.
- 430 [25] Y. Jiang, M.A. Bourebrab, N. Sid, A. Taylor, F. Collet, S. Pretot, A. Hussain, M. Ansell,  
431 M. Lawrence, Improvement of Water Resistance of Hemp Woody Substrates through  
432 Deposition of Functionalized Silica Hydrophobic Coating, while Retaining Excellent  
433 Moisture Buffering Properties, *ACS Sustain. Chem. Eng.* 6 (2018) 10151–10161.  
434 doi:10.1021/acssuschemeng.8b01475.
- 435 [26] C.A.S. Hill, A. Norton, G. Newman, The water vapor sorption behavior of natural  
436 fibers, *J. Appl. Polym. Sci.* (2009). doi:10.1002/app.29725.
- 437 [27] Y. Jiang, M. Lawrence, A. Hussain, M. Ansell, P. Walker, Comparative moisture and  
438 heat sorption properties of fibre and shiv derived from hemp and flax, *Cellulose*. 0  
439 (2018). doi:10.1007/s10570-018-2145-0.
- 440 [28] Y. Xie, C.A.S. Hill, Z. Xiao, H. Militz, C. Mai, Silane coupling agents used for natural  
441 fiber/polymer composites: A review, *Compos. Part A Appl. Sci. Manuf.* 41 (2010) 806–  
442 819. doi:10.1016/j.compositesa.2010.03.005.
- 443 [29] Y. Fujiwara, Y. Fujii, Y. Sawada, S. Okumura, Assessment of wood surface  
444 roughness: Comparison of tactile roughness and three-dimensional parameters  
445 derived using a robust Gaussian regression filter, *J. Wood Sci.* 50 (2004) 35–40.  
446 doi:10.1007/s10086-003-0529-7.
- 447 [30] L. Gurau, H. Mansfield-Williams, M. Irle, Filtering the roughness of a sanded wood  
448 surface, *Holz Als Roh - Und Werkst.* 64 (2006) 363–371. doi:10.1007/s00107-005-  
449 0089-1.
- 450 [31] B. Ugulino, R.E. Hernández, Assessment of surface properties and solvent-borne

451 coating performance of red oak wood produced by peripheral planing, *Eur. J. Wood*  
452 *Wood Prod.* (2016) 1–13. doi:10.1007/s00107-016-1090-6.

453 [32] H. Teisala, M. Tuominen, J. Kuusipalo, Superhydrophobic Coatings on Cellulose-  
454 Based Materials: Fabrication, Properties, and Applications, *Adv. Mater. Interfaces.* 1  
455 (2014) 1–20. doi:10.1002/admi.201300026.

456 [33] A. Hussain, J. Calabria-Holley, M. Lawrence, M.P. Ansell, Y. Jiang, D. Schorr, P.  
457 Blanchet, Development of novel building composites based on hemp and multi-  
458 functional silica matrix, *Compos. Part B Eng.* 156 (2018) 266–273.  
459 doi:10.1016/J.COMPOSITESB.2018.08.093.

460